PSERC

Condition Monitoring of In-Service Nonceramic Insulators and Underground Cables

Final Project Report

Power Systems Engineering Research Center

A National Science Foundation
Industry/University Cooperative Research Center
since 1996

Power Systems Engineering Research Center

Condition Monitoring of In-Service Nonceramic Insulators and Underground Cables

Final Report

R. S. Gorur, Project Leader
Arizona State University

PSERC Publication 02-25

May 2002

Information about this project

For more information about this project contact:

R. S. Gorur, Professor
Department of Electrical Engineering
Arizona State University
Tempe, AZ 85287-5706
Phone: 480-965-4894
Fax: 480-965-0745
Email: ravi.gorur@asu.edu

Power Systems Engineering Research Center

This is a project report from the Power Systems Engineering Research Center (PSERC). PSERC is a multi-university Center conducting research on challenges facing a restructuring electric power industry and educating the next generation of power engineers. More information about PSERC can be found at the Center's website: http://www.pserc.wisc.edu.

For additional information, contact:

Power Systems Engineering Research Center
Cornell University
428 Phillips Hall
Ithaca, New York 14853
Phone: 607-255-5601
Fax: 607-255-8871

Notice Concerning Copyright Material

Acknowledgements

The work described in this report was sponsored by the Power Systems Engineering Research Center (PSERC). We express our appreciation for the support provided by PSERC's industrial members and by the National Science Foundation under grant NSF EEC 0001880 received under the Industry/University Cooperative Research Center program.

The work described in Part 1 of this report was performed by a graduate student Mr. Balasubramaniam Pinnangudi. Mr. A. J. Kroese of Salt River Project, Phoenix, served as the industry and technical advisor for this part of the project.

The work described in Part 2 was performed by a graduate student Mr. Snehal Dalal. Mr. M. L. Dyer of Salt River Project, Phoenix, served as the industry and technical adviser for this part of the project.

Executive Summary

Part 1: Quantification of Corona Discharges on Polymer Insulators

Corona discharges present a serious threat to the long term performance of nonceramic (also known as composite or polymeric) insulators. To date, there has been no satisfactory method to assess the damage caused by corona in service. This project presents the first attempt to correlate visible patterns of corona discharges on actual insulators with the energy associated with the discharge. An UV camera capable of capturing the corona discharge even during daytime has been employed. Conventional partial discharge (PD) monitoring has been used to assess the magnitude of corona in a well-shielded high voltage laboratory. An image processing technique that converts the light signal into quantifiable measures (pixel intensity and area) has been attempted.

The results from this project indicate that there is a correlation between the visible pattern of corona, measured discharge energy and the pixel intensity and area. This correlation has been proven under both dry and wet conditions. It appears that data of the threshold corona energy intensity to cause deterioration of the housing material (obtained from previous projects) can be used to predict the performance of nonceramic insulators under actual service conditions. This project has considered those nonceramic insulators that do not have any manufacturing or design defects. The next phase of the project will involve the evaluation of defective insulators.

Part 2: Prediction of Future Performance of In Service XLPE Cables

This study examines the performance of 15kV XLPE new and aged cable (taken out from the service after 10 + years) in context with electrical tree and electrical failure of cable. The breakdown tests are preformed using needle-plane geometry at room temperature as well as elevated temperature of 100^0C. A statistical technique like regression analysis is utilized to analyze the test results as well as to predict the future performance and life expectancy of cables. The analytical techniques like Fourier Transform Infra-Red (FTIR) spectroscopy is used to study the permanent changes in the XLPE material. This project proves the fact that there are permanent changes occurring in the material that lead to progressive degradation and/or failure in the long run.

A number of conclusions have been reached in this project.

- After aging of around 10 years in dry weather like that of Arizona, cable performance is degraded by at least 25%.
- As the slope of the both new and aged cable model remains same, it can be concluded that the rate of degradation is not changing with the age of the cable.
- A different depth of penetration (damage due to accidental dig ins) is required to failure for aged and new cable. For new cable it is approximately 5.9 mm and for aged cable it is 3.8 mm. It can be concluded from this that aged cable are more susceptible to failure due to accidental dig ins.
- In XLPE samples, reduction in the absorption bands due to $[-CH_2-CH_2]_n$ at 2840 cm^{-1} to 2915 cm^{-1} on the surface can be identified in FTIR spectrums.
- CH_2-CH_2 is the backbone of XLPE material and reduction of this backbone material is noted with aging as well as after electrical failure. Side chain absorption band made up of CO= and – CH_2 at 1460 cm^{-1} also decreases and reaches higher transmittance level (lower absorbance level) than case of new cable without failure.
- The ATH-related absorption band ($\leq$ 1020 cm^{-1}) is reduced as the age of cable increases and also with the failure of the cable

Table of Contents

Part 1 Quantification of Corona Discharges on Polymer Insulators

1.1 Introduction

Corona can be initiated on non-ceramic insulators (NCI) due to defective manufacturing and deficiencies in hardware design. Corona can cause premature failure. To aid in proper insulator selection, it is important to determine the magnitude of corona and the damage threshold of various insulator-housing materials. In this project, interesting pre-flashover activities that are related to corona are observed on polymer insulators subjected to high voltage. The electrical activities that occur during bursts of light emission have been monitored. A high-speed UV camera has been used for visual observations.

The high-speed corona camera detects and locates weak corona signals by overlaying a UV video image of the corona on a visible video image of the background. The solar blindness is achieved by using a special filter that is transparent in the solar blind UV band and is completely opaque to the solar radiation.

Image processing techniques are used to measure the brightness of the discharge in terms of the pixel illumination levels. A correlation is drawn between the image obtained with a corona detection camera and the energy associated, as measured by traditional partial discharge (PD) detection methods. Critical values of energy, and the associated visual patterns beyond which the corona has a deteriorating influence on the insulator have been determined. This provides an effective way to predict the severity of corona on the insulator in-service from ground inspection. Simulation results are reported, together with discussion of various problems

1.2 Experiment Setup

The experiment setup is shown in Figure 1. The closed loop includes power supplier, insulator sample, coupling capacitor, coupling quadripole, high-speed corona camera and PD detector.

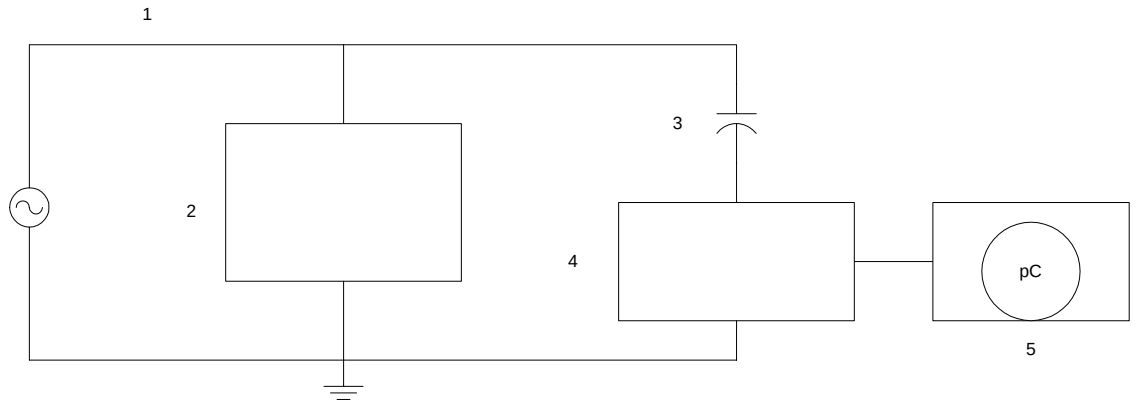

Figure 1: Schematic of a PD measuring system

1) High voltage
2) Test object
3) Coupling capacitor
4) Coupling quadripole
5) PD measuring instrument

Partial discharges in high-voltage systems are local electrical discharges within the insulation of these systems. If these partial discharges reach a certain level, they can cause permanent damage to the insulation. For this reason a correlation is established between the magnitude of partial discharge (in pC) and the life expectancy of the insulation.

The high-frequency unipolar PD impulse is picked up with the coupling quadripole (CQ) and routed to the detector using the measuring cable. The detector can be used either in the straightforward method or in a bridge circuit. The apparent charge is measured in the detector by quasi-integration in pre-selectable frequency ranges.

The following devices are needed to perform PD measurements:

- PD Detector, which amplifies the PD impulses and displays the magnitude on a oscilloscope
- Coupling quadripole with which the PD signal is sensed

- Coupling capacitor, which decouples the high frequency PD impulses from the high voltage
- Calibrator, which supplies the calibrating impulses with a defined charge

Visual observation of corona is difficult because it emits weak radiation, mostly in the ultra-violet (UV) spectral range, and is virtually invisible except in darkness as shown in Figure 2.

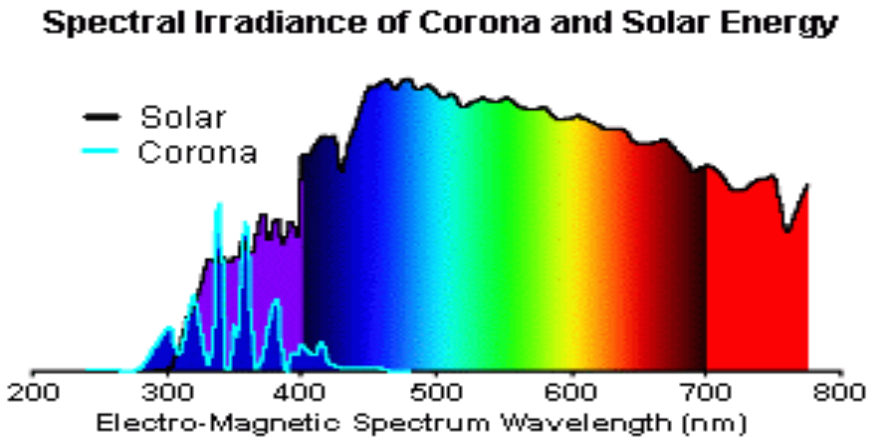

Figure 2: Corona Spectrum

The corona emission in air peaks around 300-360 nm, but solar radiation in this region is much stronger than the corona. In the "solar blind" region (240-280 nm) the emission is much weaker but the solar background is negligible. A special filter that transmits light between 240-280 nm and completely blocks longer wavelengths is combined with a photon-counting intensified charge coupled devices (CCD) so that it responds only to the corona emission spectrum. The optical system transmits the same scene to the visible-light camera enabling it to present a view of the source of the discharge in perfect registration, without parallax.

1.3 Test Procedures

The insulator is subjected to high-voltage, beginning with 10 KV. The voltage is increased in steps of 5 KV until the first discharge is observed on the insulator surface. The magnitude of discharge is determined by using the conventional PD detector. As the voltage is increased further, the discharge magnitude and intensity are observed to increase as shown in

Figure 3 and 4. The readings are tabulated and the above test procedure is repeated on different samples to study the partial discharge patterns.

Figure 3: Corona at 50 KV of discharge magnitude 30 pC

The high-speed photography of the pre-flashover events is performed in conjunction with the above diagnostics. The streak photography of the initiation part involves problems in coincidence of timing between the trigger of the camera unit and the discharge event. The observed photograph frames, synchronized with the partial discharge data to facilitate comparison.

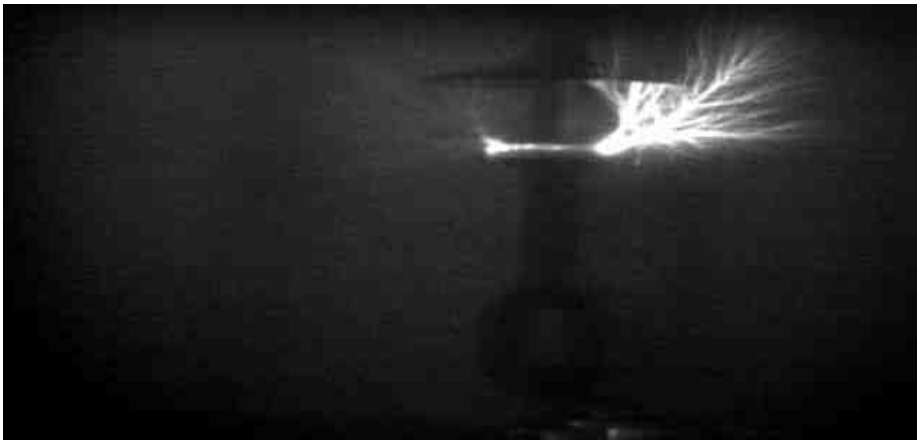

Figure 4: Corona at 80 KV of discharge magnitude 3.0 nC

1.4 Image Analysis and Processing

The images captured during the pre-flashover events are stored in the memory banks of the IBM PC. The images required a number of processing and noise removal steps to present them in a form suitable for mathematical manipulation and quantitative analysis. The JPG files are converted into binary format by using the image processing tools available in MATLAB. It may be noted that the binary file represents the light intensity levels at different locations of the image matrix. The elements of the image matrix are summed up by using a computer program to give the total intensity of the captured image. The plot (intensity vs. pixel number) thus obtained are compared with the corresponding partial discharge values and analyzed. The captured images are associated with inaccuracies caused by pollution from the backlight system, microscopic dust particles surrounding the sample as shown in Figure 5. The processed image is the end result of a series of processing steps designed to realize a "clean" image as shown in Figure 6.

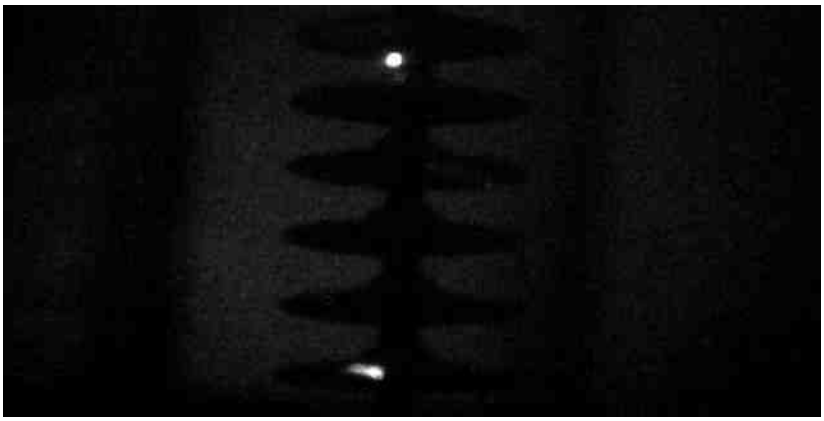

Figure 5: Corona Image on a polymer insulator

Figure 6: Clean Image after processing

Parameter Extraction

(1) Radial Extent, r

Simply calculated by finding the tree or light emission pixel (x_i, y_i) in the processed image array that is farthest from center of discharge, (x_c, y_c)

$$r = \sqrt{((x_i - x_c)^2 + (y_i - y_c)^2)}$$

(2) Area growth, A

Area is calculated by counting all the pixels that are part of the pre-flashover discharge or light emission spectrum. The CCD pixel is a square of approximately 4.3 μm. Area is therefore obtained by multiplying the area of a single pixel with the number of illuminated pixels.

(3) Light intensity, I

Light intensity is calculated by performing a weighted sum on all the pixels that are part of the light emission spectrum. The pixel intensity is measured relative to the previously calculated base noise level. The intensity values are normally weighted with reference to this base level.

$$I = \sum_{n=1}^{N} I_{pixel} - I_{base}$$

where N is the number of pixels in the region of interest.

1.5 Partial Discharge Parameters

The total charge is defined as the sum of the magnitudes of all PD pulses detected during a single ac cycle. It is calculated at each time step through the lifetime of the sample. The maximum discharge magnitude detected during any given period of data acquisition increases during the lifetime of the discharge. This suggests a relation between the discharge radial extent, area and intensity with the partial discharge magnitude. However, it should be noted that the maximum discharge magnitude is not just a function of the above parameters, but also of applied voltage/field strength.

1.6 Test Results

With increase in the corona discharge magnitude, the area under the intensity plot is increased as shown as in Figure 8 and 11. By using MATLAB programming the overall intensity is calculated for various discharge magnitudes which provides an effectively way to determine the discharge energy associated by ground inspection.

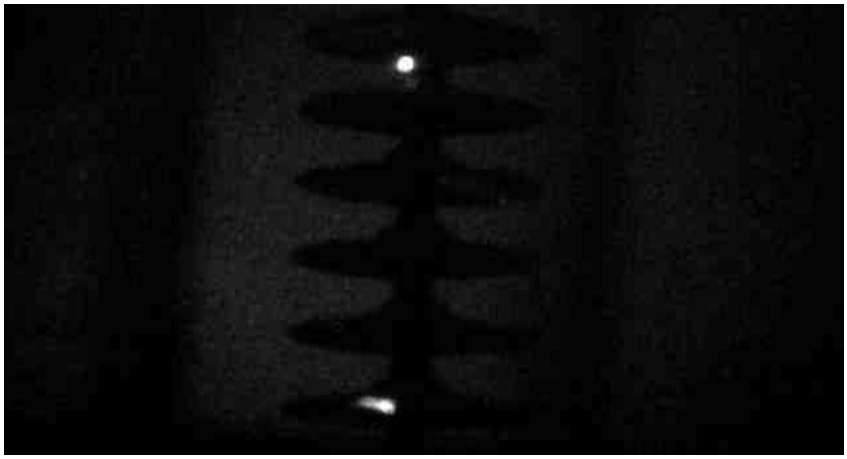

Figure 7: Discharge on a EPDM-Alloy type nonceramic insulator sample at 80 KV

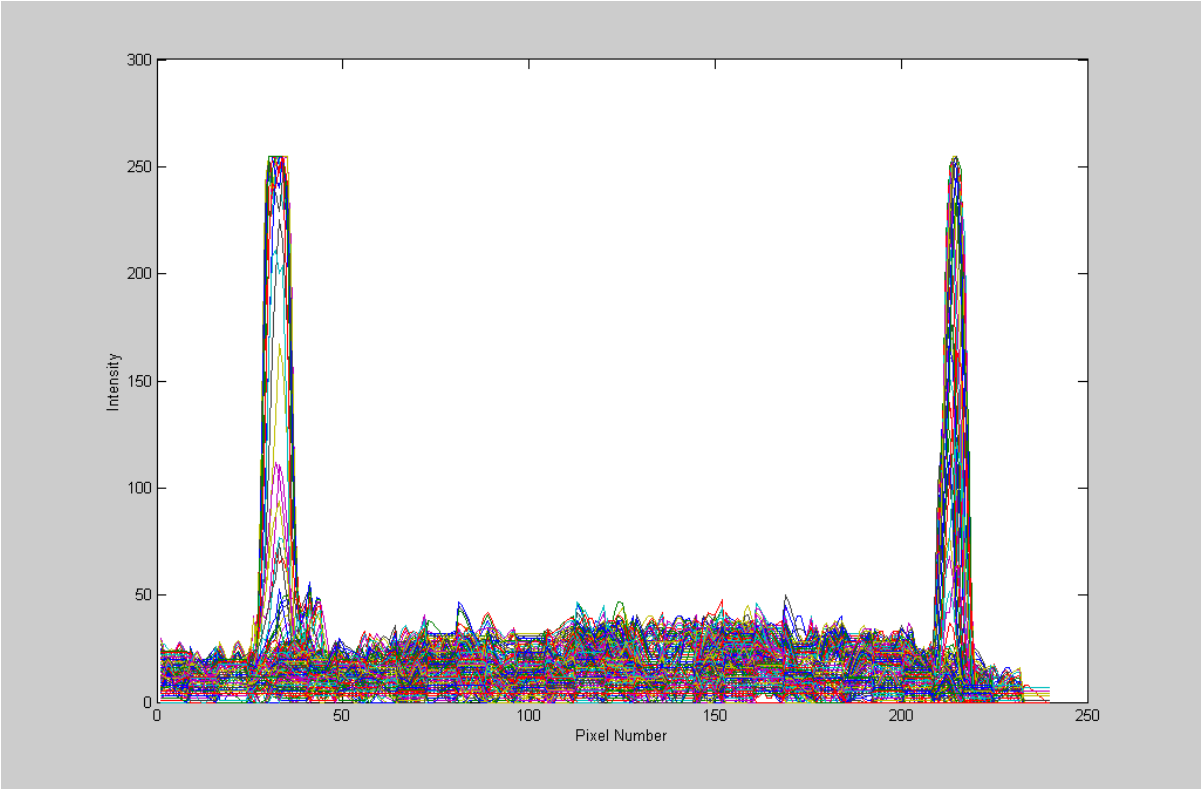

Figure 8: Intensity Plot for discharge magnitude of 2.0 nC

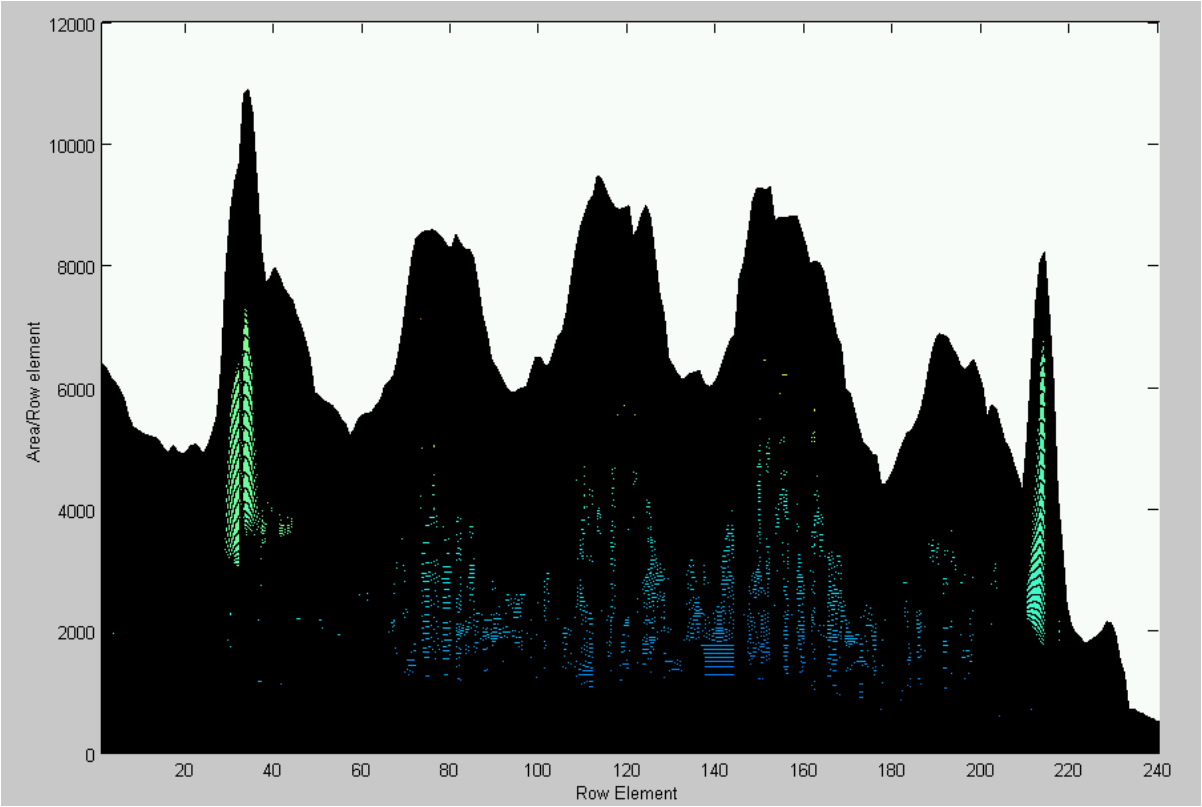

Figure 9: Discharge area for magnitude of 2 nC

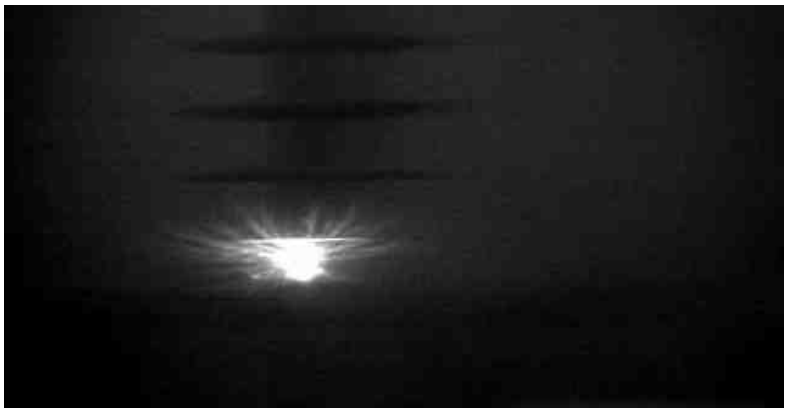

Figure 10: Discharge on a silicone rubber type nonceramic insulator at 80 KV

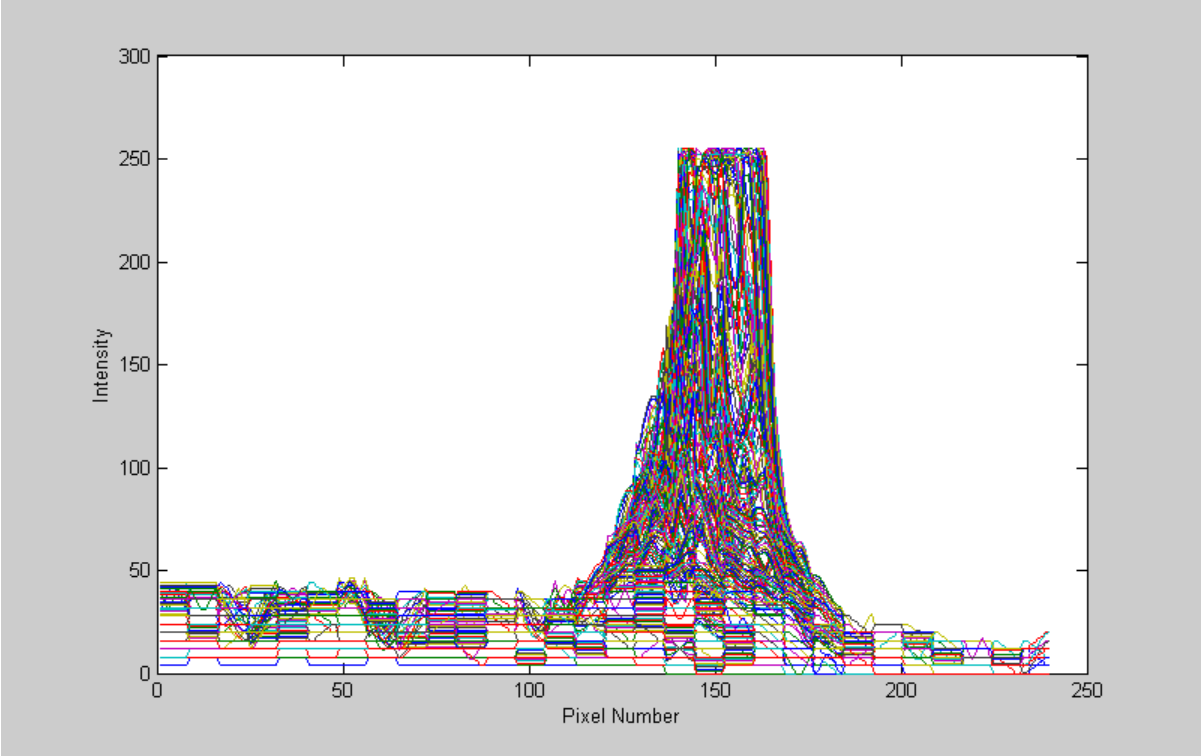

Figure 11: Intensity plot for discharge magnitude of 4.9 nC

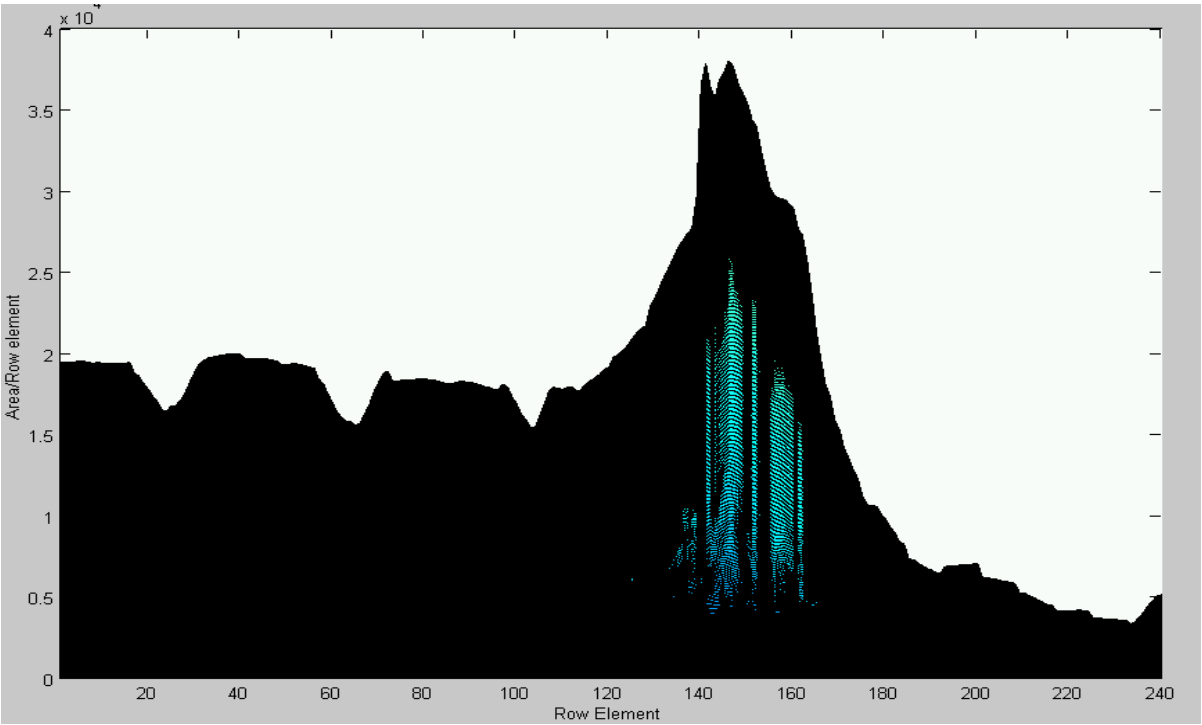

Figure 12: Discharge Area for magnitude of 4.9 nC

1.7 Future Work

Preliminary investigations indicated a correlation between the visual corona discharge patterns and their corresponding energies under dry conditions. Future research would target at extending the correlation and testing its validity for different atmospheric conditions.

1.8 References

[1] Moreno, V.M.; Gorur, R.S.; "Effect of Long-Term Corona on Nonceramic Outdoor Insulator Housing Materials," IEEE Trans. on Dielectrics and Electrical Insulation, Vol. 8, No.1, pp. 117-128, 2001.

[2] Moreno, V.M.; Gorur, R.S.; "Ac and Dc Performance of Polymeric Housing Materials for HV Outdoor Insulators," IEEE Trans. on Dielectrics and Electrical Insulation, Vol. 5, No. 3, pp. 342-350, 1999.

[3] Hackam, R.; "Review: Outdoor HV Composite Polymeric Insulators," IEEE Trans. on Dielectrics and Electrical Insulation, Vol. 6, No. 5, pp. 557-585, 1999.

[4] Starr, W.T.; "Polymeric Outdoor Insulation," IEEE Trans. on Electrical Insulation Vol. 25, No. 1, 1990.

[5] Hall, J.F.; "History and Bibliography of Polymeric Insulators for Outdoor Applications," IEEE Trans. on Power Delivery, Vol. 8, No. 1, 1993.

[6] Yoshimura, N.; Kumugai, S.; Nishimura, S.; "Electrical and Environmental Aging of Silicone Rubber used for Outdoor Insulation," IEEE Trans. on Dielectrics and Electrical Insulation, Vol. 6, No. 5, pp. 632-650, 1999.

[7] Karady, G.G.; Shah, M.; Brown, R.L.; "Flashover Mechanism of Silicone Rubber Insulators used for Outdoor Insulation - I," IEEE Trans. on Power Delivery, Vol. 10, No. 4, pp. 1965-1971, 1995.

Part 2 Prediction of Future Performance of In Service XLPE Cables

2.1 Introduction

The beginning of power cable technology can be traced back up to 1880s, when the incandescent light was introduced. Solid polyethylene extruded insulated power cables were first introduced in 1950s. It became apparent after few years of service that all types of polyethylene are susceptible to degradation and eventual failure under the conditions imposed by electrical stress in a service environment. The changes in polymeric insulation that lead to electrical failure fall into two interrelated categories, molecular level degradation and microscopic changes [1]. At molecular level reactions occur that change the chemical nature of polymer molecules. The microscopic changes include phenomena such as tree growth, void formation, cracks and crazing [2]. A common cause for underground residential distribution (URD) power cable failure is the formation and growth of water trees and electrical trees.

This report is organized as follows. Section 2.2 discusses in brief parameters and various mechanisms for initiation and propagation of electrical tree suggested till date. Section 2.3 discusses the experimental set up and data monitored during electrical breakdown test and FTIR spectroscopy test. Section 2.44 discusses the result obtained from breakdown test as well as FTIR test. In section 2.5, regression analysis applied to the results obtained from breakdown test, and conclusion is discussed. Section 2.6, gives scope of future work.

2.2 Physics of Treeing

Tree is defined as '*latent damage in the insulation that consists of microscopic channels formed by partial breakdown of defective or overstressed region*' and as '*hollow tubes with non conducting walls and containing the gaseous products of discharge*' [3]. Trees are classified based on different criteria such as shape of the trees, location of origination or characteristics, out of which most accepted classification of trees comes based on its characteristics as electrical (dry) and water (wet) tree. The main difference between electrical and water tree emphasized is based on presence of hollow channel. Electrical tree consist of hollow channel resulting from the decomposition of material, which is clearly visible in translucent or transparent solid dielectrics when examined with an optical microscope and transmitted light.

Electrical treeing has three distinct phases. The first is the initiation phase, or the incubation period, during which no detectable partial discharge occur. The second is the growth of propagation phase during which the tree propagates by continuous or periodic partial discharge activity. The third is breakdown phase, during which cable insulation fails due to dielectric breakdown. There are different mechanisms proposed for initiation of electrical tree. in [4], which includes formation of electrical tree due to electrical tree, hot electron and mechanical stress. Growth of electrical tree is defined [5] as, an array of fine (~1 μm diameter) erosion channels form through a partial discharge (PD) activity within the evolving tree structure. These partial discharges cause decomposition of the insulation, mainly in the gases. The composition of produced gases depends on material and local temperature produced by the discharge. All researchers seem to agree upon the fact that once initiated, electrical tree will propagate through the weakest part of the structure due to effect of discharge in the formed cavity. At higher temperature due to reduction in intrinsic strength, time to breakdown is reduced by considerable amount. This work attempts to predict the future performance of cable based on breakdown characteristic of the insulation implementing real working condition of the cable with temperature of 100^0C.

2.3 Experimental Setup

2.3.1 Electrical Breakdown Test

Since electrical trees are initiated at, and grow from sites of stress concentration rather than in uniform fields, it is important that selected experimental procedure provide constant and reproducible conditions of electrical stressing. Among the different experimental procedures mentioned in [6], the needle test is selected, based on ASTM D 3756-97. The needle test provides comparative data and not the degree of correlation with actual performance in service, which is the main focus of this work. The procedure of test involves the placing of needle of carefully controlled and identical geometry into a compression-molded block of polymer as shown in Figure 1. The test set up geometry consists of mainly two parts, namely the holding compartment and the needle driver. The holding compartment is a Plexiglas cubicle designed to support samples with diameters up to 4.5 cm (~1.75 in). The needle driver is a ¼-28 machined screw designed to impel a drill blank (needle) inside the samples. To measure the depth of penetration of the needle inside the samples, dial caliper is used as shown in Figure 2. The depth of penetration is calculated by subtracting the initial and final position readings from the dial caliper.

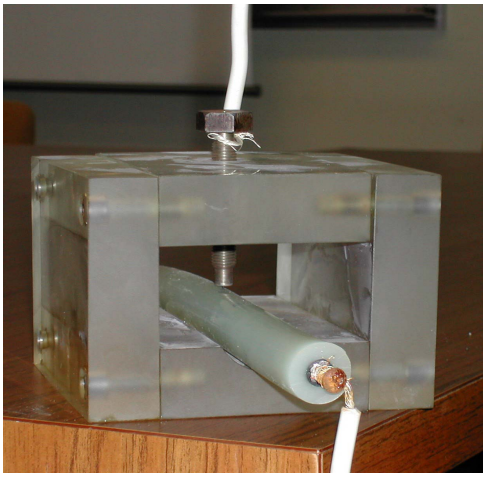

Figure 1 Test Setup Geometry

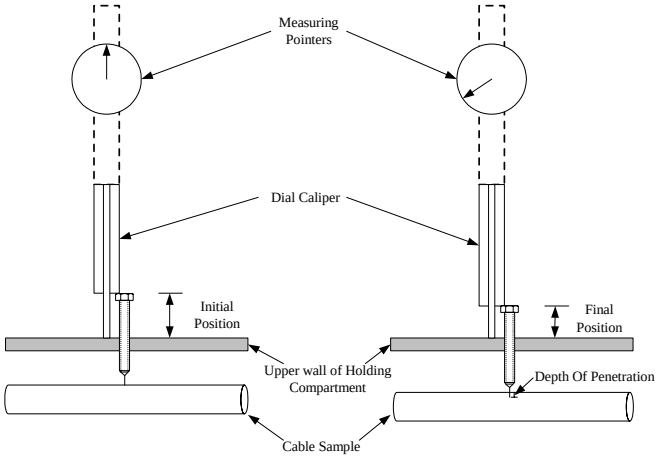

Figure 2 Measurement of Depth of Penetration

Such geometry gives a stress enhancement that can be calculated, under the assumption of a hyperbolic shape of the tip, by means of the relation given in [7] as:

$$E_{max} = \frac{2 \times V}{r \times ln\left(4d/r\right)} \quad (1)$$

Where, E_{max} = electrical field on the tip of the needle
d = interelectrode gap
r = Tip radius
v = Applied voltage

In every case , the needle is first cleaned by alcohol and then inserted very slowly in the insulation to eliminate residual stress or fracturing of the specimen material. A high voltage is applied to the needle while grounding conductor of the cable as shown in Figure 3. Experiments are performed at various depths of needle penetration and with various voltage patterns as discussed in next section.

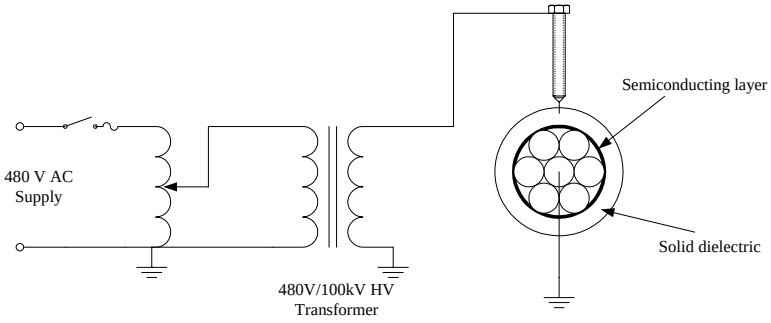

Figure 3 Electrical Circuit for Breakdown Test

During the electrical breakdown test the following data are closely monitored.

- Depth of penetration of needle in the insulation
- Voltage applied in kV.
- Time to breakdown failure in minutes.
- Cause of failure by visual inspection, whether it was flashover or puncture of the insulation.

2.3.2 FTIR Spectroscopy Test

FTIR has proven to be useful in studying and monitoring the structural changes in dielectric materials before and after being subjected to different kind of stresses and aging and has been used extensively. In order to investigate generation of any new material and the chemical changes in XLPE insulation due to aging as well as due to dielectric failure, corresponding samples have been tested to get the intensity spectrums. The obtained spectrums are analyzed

based on the intensity of peaks. A Nicolet 205 FTIR spectrometer equipped with an EZ-scope attachment from Spectra-Tech is used as a mean of microanalysis. The detector used is a liquid nitrogen cooled MCT (Mercury Cadmium Telluride) detector.

The polyethylene is a polymeric material with long chain of hydrocarbon plastic produced by the polymerization of ethylene gas (C_2H_4) either under low or high pressure. The polyethylene can be classified based on relative degree of branching (side chain formation) in their molecular structures, which can be controlled with selective catalysts. The cross-linking process causes PE to change from a thermoplastic to thermosetting material with a marked improvement in both physical and electrical properties. The individual molecular chains are bonded to each other to form a three-dimensional polymer of extremely high molecular weight in XLPE. Carbon black is added in XLPE to increase tensile strength and hardness but at the same time affects the electrical properties of the insulation. Carbon black is added to guard against ultraviolet radiation, which due to its absorption by the carbonyl group (C=O) may induce degradation [8].

2.4 Results

2.4.1 Electrical Breakdown Test

Experiments are done at 100^0C to simulate the actual working conditions of the cable. Initially to finalize the voltage pattern for the electrical breakdown test, a continuously increasing high voltage is applied with different depth of penetration and breakdown voltage is recorded. Ten different samples of new type have been tested as shown in Table 1. Average breakdown voltage was about 20.64 kV with average depth of penetration of 2.68 mm. Using this result the voltage pattern decided is 20 kV for first hour and then 5 kV increasing voltage per every half an hour thereafter. The results obtained from the voltage pattern described have been evaluated with the concept of total energy required to failure. The Voltage-Time product is calculated for each case and attempt is made to relate this with the various depth of penetration and temperature.

Table 1 Breakdown Voltages for New Cables

(Continuously increasing nature)

Sample Number	**Breakdown Voltage (kV)**	**Depth of Penetration in mm**
1	15	5.00
2	26	3.20
3	10	1.65
4	20	3.30
5	32	0.91
6	26	3.78
7	13	3.04
8	33	3.30
9	32	2.83
10	20	2.46
Average	20.64	2.68

A similar approach has been adopted for the aged cables. The final energy required to breakdown is noted. Table 2 & 3 shows the results of electrical breakdown test for new cables and aged cables respectively. In Table 2 and 3, the failure to flashover is not included but the same is included in Figure 4. Figure 4 indicates the results of Table 2 & 3 in the form of graphs with inclusion of cases where breakdown occurred. Apart from data presented here, large numbers of experiments are done to prove that Voltage-Time product is constant for the same depth of penetration and different voltage patterns. The graph shown in Figure 4, clearly indicates degradation in the cable due to aging. By extrapolating the graph of Figure 4, the future performance of the cable can be predicted with some constraints. A linear regression analysis applied to the obtained data to formulize the equation, which is discussed in next section.

Table 2

Electrical Breakdown Test for New Cable

(At 100^0C)

Sample Number	Depth of Penetration in mm	KV-Time Product (kV-min)
1	3.556	1500
2	4.572	1950
3	4.572	1200
4	4.064	1930
5	3.302	3588
6	3.683	1800
7	3.302	3429
8	4.064	2625
9	3.556	2340
10	4.191	1880

Table 3

Electrical Breakdown Test for Aged Cable

(At 100^0C)

Sample Number	Depth of Penetration in mm	KV-Time Product (kV-min)
1	2.54	1950
2	3.302	400
3	3.175	625
4	2.794	875
5	3.556	500
6	3.302	680
7	3.429	750
8	3.048	720
9	2.667	1200
10	2.794	1800

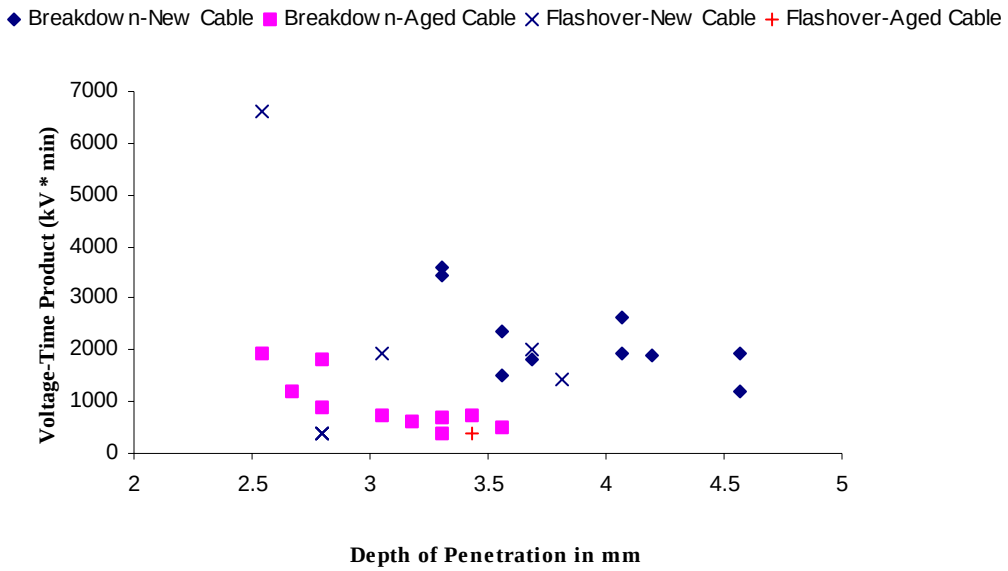

Figure 4 Electrical Breakdown Test Data

2.4.2 FTIR Spectroscopy Test

One of the aims of the study is to analyze FTIR spectra in order to shed light and to understand the permanent changes occurring in XLPE insulating material. Typical FTIR spectra are recorded for each of the sample after electrical breakdown test. There was a significant change in the FTIR spectrums for new cables, aged cables and failed cables. No significant change was observed in the FTIR spectrums with respect variation in depth of penetration or voltage-time product. Figure 5 shows typical FTIR spectra for New, aged and failed cable sample stacked together. Figure 6 shows the same FTIR spectra stacked differently.

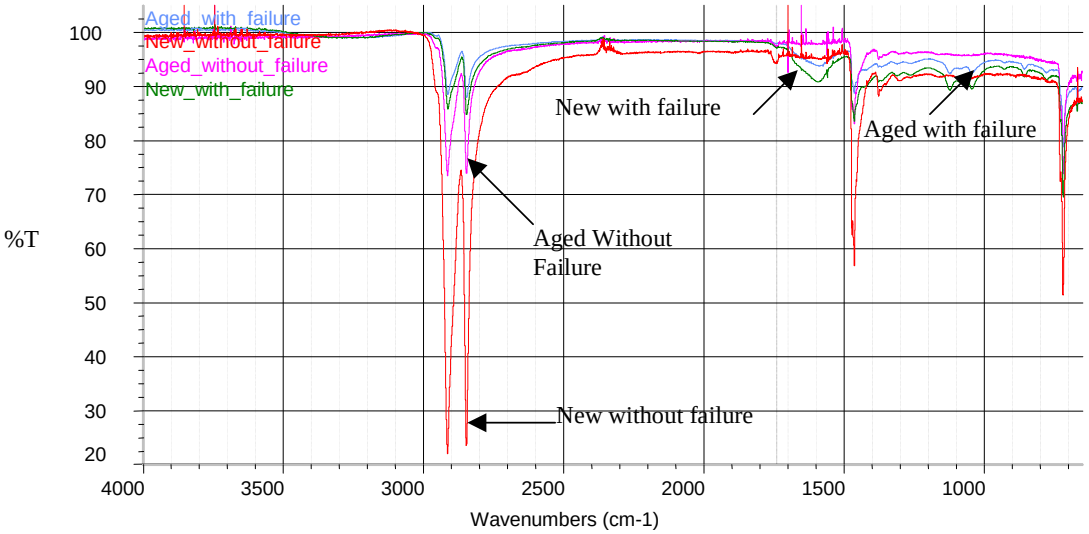

Figure 5 FTIR Spectra of XLPE cables for new, aged, unfailed and failed samples

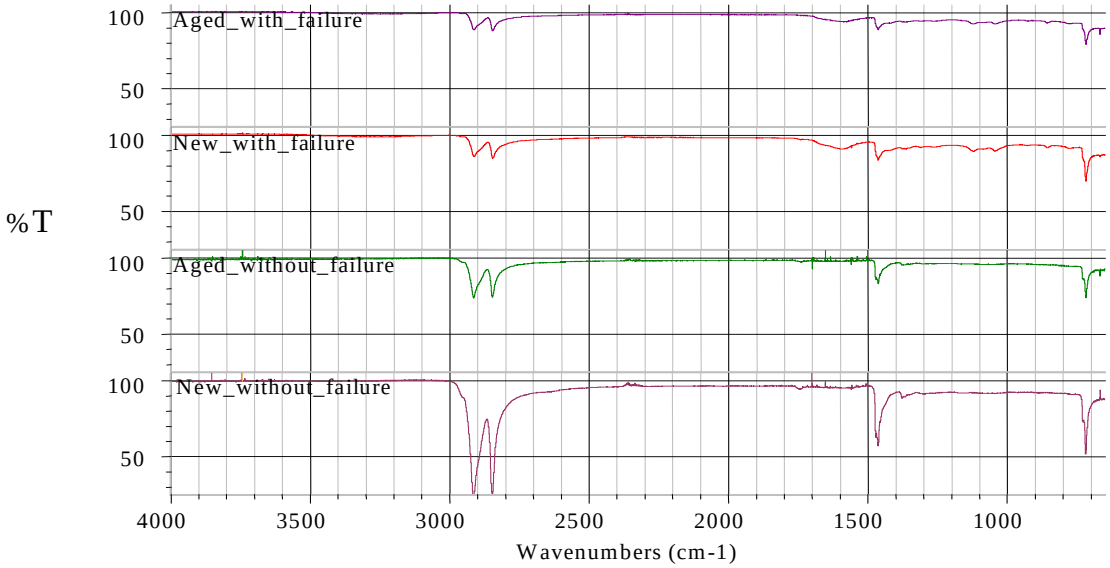

Figure 6 FTIR Spectra of new and aged XLPE cables

The strength of the absorption bands due to any chemical group is proportional to its concentration within the material [9]. By examining the FTIR spectra, it was observed that peak height at different wavelengths varied with age of the cable and also with the failed samples and healthy samples. It is well known that changes in IR absorption peak heights may be due to actual changes in the chemical composition of the XLPE.

2.5 Regression Analysis

Minitab® statistical software has been used extensively in this project. By investigating Figure 4, one notices that there are clear different trend lines for the New and Aged cables. The least square estimates of the intercept and the slope of the simple linear regression model for new and aged are provided in Table 4 and Table 5. Figures 7 and 8 show the regression plots with the scattered data points. Figures 8 and 10 show the regression plots with 95% confidence and prediction intervals for new and aged cables. The model of new cable is presented by equation 2, while equation 3 represents aged cable model.

$$\text{kV-Minute Product}_{\text{New}} = 6404 - 1075.4 \times \text{Depth of Penetration in mm} \quad (2)$$

$$\text{kV-Minute Product}_{\text{Aged}} = 4792 - 1255.3 \times \text{Depth of Penetration in mm} \quad (3)$$

Table 4 Results of the regression analysis for New Cable

Predictor	**Coefficient**	**Standard Deviation**	**t-test**	**P Value**
Constant	6404	1723	3.72	0.006
Slope	-1075.4	440.5	-2.44	0.040

Table 5 Analysis of variance (ANOVA) results for New Cables

Source	Degrees of freedom	Sum of Squares	Mean Square	F	P Value
Depth of Penetration	5	4630951	926190	4.17	0.096
Error	4	888203	222051		
Total	9	5519154			

Table 6 Results of the regression analysis for Aged Cable

Predictor	Coefficient	Standard Deviation	t-test	P Value
Constant	4792	975.5	4.91	0.001
Slope	-1255.3	316.9	-3.96	0.004

Table 7 Analysis of variance (ANOVA) results for Aged Cables

Source	Degrees of freedom	Sum of Squares	Mean Square	F	P Value
Depth of Penetration	7	2100038	300005	1.28	0.505
Error	2	467013	233506		
Total	9	2567050			

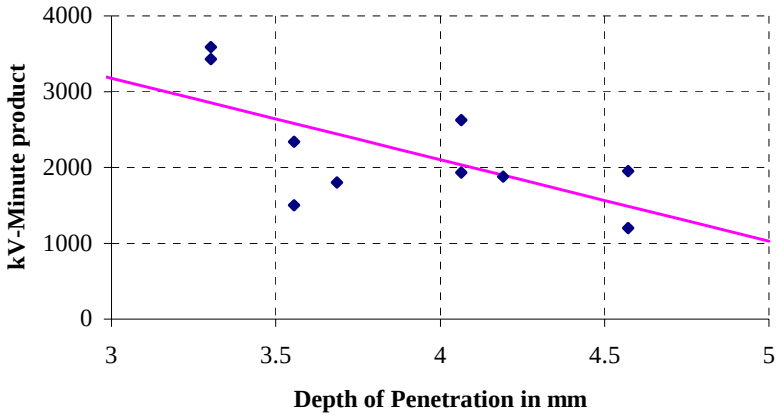

Figure 7 Regression Line with data for New Cable

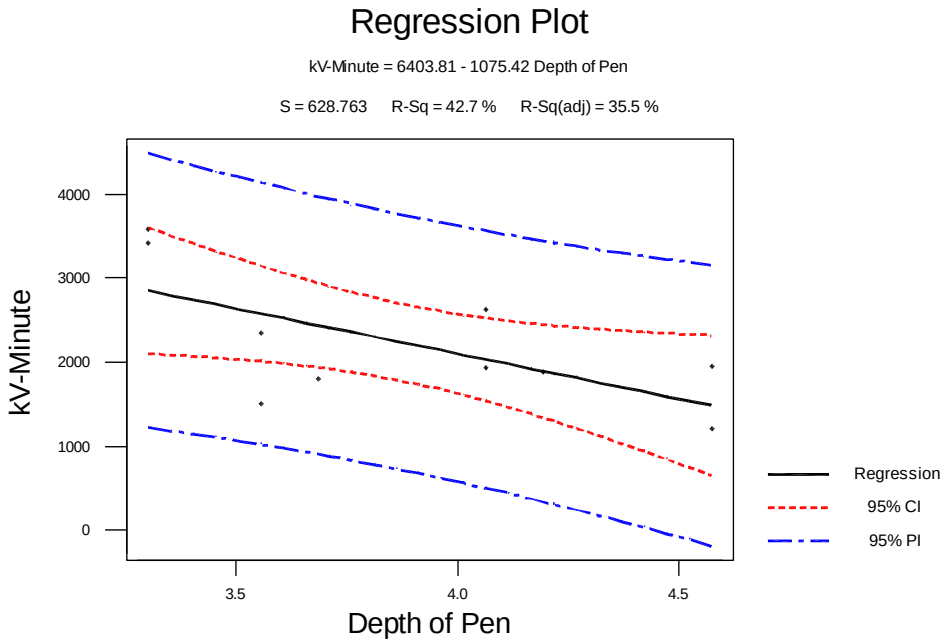

Figure 8 Regression plot, Confidence and Prediction Limits for new cable

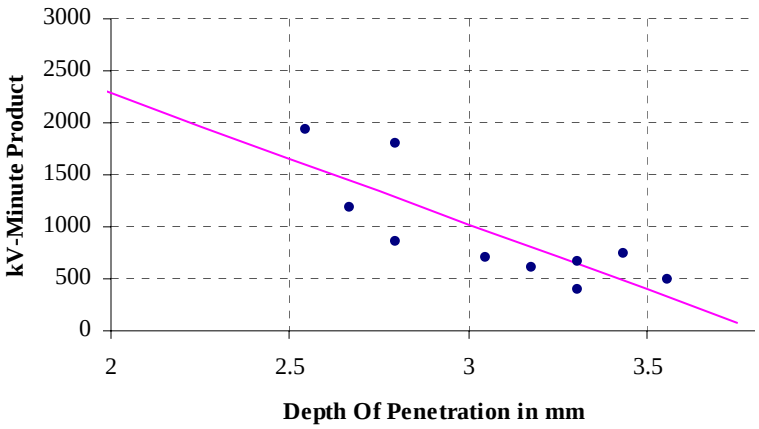

Figure 9 Regression Line with data for aged Cable

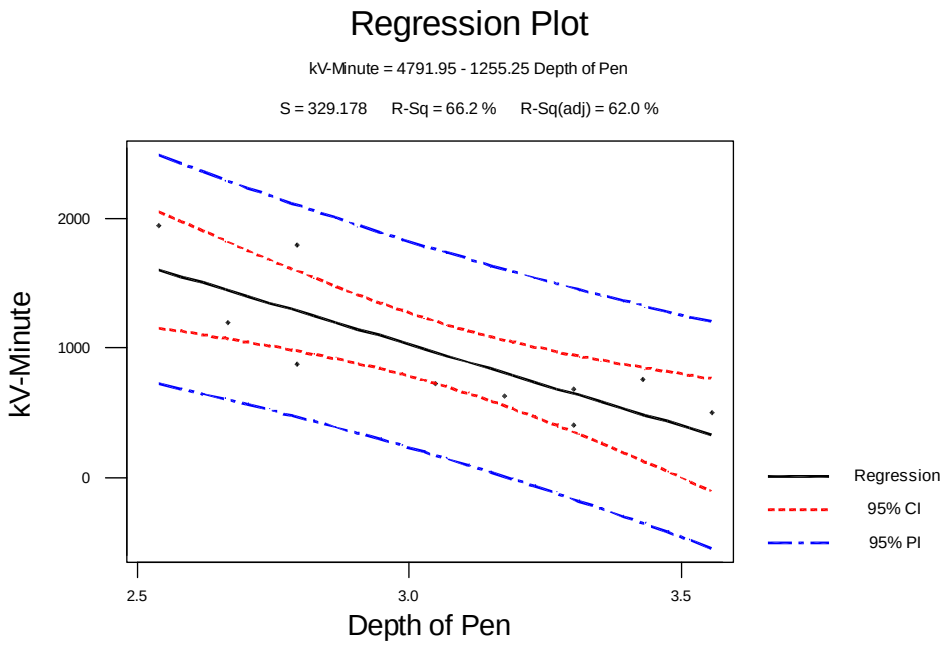

Figure 10 Regression plot, Confidence and Prediction Limits for aged cable

2.6 Conclusion

- By examining equations 2 and 3, it can be concluded that after aging of around 10 years in dry weather like that of Arizona state of USA, cable performance is degraded by at least 25%.
- As the slope of the both new and aged cable model remains same, it can be concluded that the rate of degradation is not changing with the age of the cable.
- A different depth of penetration (damage due to accidental dig ins) is required to get zero kV-Minute product for aged and new cable. For new cable it is approximately 5.9 mm and for aged cable it is 3.8 mm. It can be concluded from this that aged cable are more susceptible to failure due to accidental dig ins.
- In XLPE samples, reduction in the absorption bands due to $[-CH_2-CH_2]_n$ at 2840 cm^{-1} to 2915 cm^{-1} on the surface can be identified in FTIR spectrums.
- CH_2-CH_2 is the backbone of XLPE material and reduction of this backbone material is noted with aging as well as after electrical failure. Side chain absorption band made up of CO= and – CH_2 at 1460 cm^{-1} also decreases and reaches higher transmittance level (lower absorbance level) than case of new cable without failure.
- The ATH-related absorption band ($\leq$ 1020 cm^{-1}) is reduced as the age of cable increases and also with the failure of the cable.

2.7 Future Work

The following work can be done in future to fully understand the change in breakdown strength of the aged cables.

- Similar experiments can be done on cables of different in-service age and degradation in the breakdown characteristics can be examined.
- Study can be repeated with different temperatures, depending upon actual working conditions of the cables.
- This study involves cables used in dry weather condition, similar approach can be extended to the cables installed under different environmental conditions.

2.8 References

[1] Bartnikas, R.: *Engineering Dielectrics Vol. IIB, Electrical properties of solid insulating materials: Measurement techniques*, ASTM Special Technical Publication 926, Philadelphia, 1987.

[2] Eager, G. S. Jr., Katz, C., Fryszczyn, B., Fischer, F. E., Thalmann, E.: "Extending service life of installed 15-35kV extruded dielectric cables," IEEE transactions on power apparatus and systems, Vol. PAS-103, No. 8, August 1984, pp. 1997-2005.

[3] Vahlstrom, W. Jr.: "Investigation of insulation deterioration in 15kV and 22kV polyethylene cables removed from service", IEEE Transactions on power apparatus and systems, Vol. PAS-91, May/June 1972, No. 3, pp. 1023-1028.

[4] Bulinski, A. T., Bamji, S. S., and Densley, R. J.: "Factors affecting the transition from a water tree to an electrical tree," Electrical Insulation, 1988, Conference Record of the 1988 IEEE International Symposium on, 1988, pp. 327-330.

[5] Champion, J. V., Dodd, S. J., Zhao, Y., Vaughan, A. S., Brown, M., Davies, A. E.: Sutton, S. J., and Swingler, S. G.: "Mophology and the growth of Electrical Trees in a Propylene/Ethylene Copolymer," IEEE Transactions on Dielectrics and Electrical Insulation, Vol. 8, No. 2, pp. 284-292, April 2001.

[6] Bartnikas, R.: *Engineering Dielectrics Vol. IIA, Electrical properties of solid insulating material: Molecular structure and electrical behavior*, ASTM Special Technical Publication 783, Philadelphia, 1983.

[7] Bozzo, R., and Sierota, A.: "Contribution to the testing of treeing inception in needle arrangements manufactured by different methods," Conference record of 1988 IEEE international symposium on Electrical Insulation, Boston, MA, June 5-8, 1988, pp. 351-354.

[8] Bartnikas, R., and Drivastava, K. D.: *Power and Communication Cables, Theory and Applications*, IEEE Press, New York, 1999.

[9] Gorur, R. S.; Karady, G. C.; Jagota, A.; Shah, M. and Yates, A. M.: "Aging in Silicone Rubber used for Outdoor Insulation", IEEE Transactions on Power Delivery, Vol. 7, No. 2, April 1992, pp. 525-538.